# Measures of Stability for Roofs over Cavities in Rock

Radoslaw L. Michalowski, Ph.D., F.ASCE<sup>1</sup>; and Dowon Park, Ph.D.<sup>2</sup>

<sup>1</sup>Dept. of Civil and Environmental Engineering, Univ. of Michigan, Ann Arbor, MI.

Email: rlmich@umich.edu

<sup>2</sup>Dept. of Civil Engineering, Univ. of Seoul, Dongdaemun-gu, Seoul, South Korea.

Email: dowon@uos.ac.kr

## **ABSTRACT**

Engineered cavities in rock formations are often part of an underground transportation infrastructure. Three measures of roof stability in such cavities are discussed: the stability number, the factor of safety, and the support pressure needed to prevent cavity roof failure in weak rock. The stability number is a dimensionless combination of the rock properties and the size of the cavity when roof failure becomes imminent. While there exists substantial experience in application of the stability number and the factor of safety to soil structures, their use to define the safety of rock structures is intricate. This is because the strength envelope for rocks is a non-linear function of the mean stress. The specific function used in the analysis is the Hoek-Brown failure criterion. The kinematic approach of limit analysis is used, and the results are presented in charts. All measures of stability are strongly dependent on the Geological Strength Index, and, to a lesser degree, on other parameters in the Hoek-Brown failure criterion.

# INTRODUCTION

Development of underground infrastructure presents challenges, particularly when large-span cavities need to be constructed in weak rock. A typical example of underground space development are tunnels with either curved or flat ceilings that may be susceptible to roof failures. Stability of roofs in deep cavities is considered in this presentation. Deep cavities are those where the roof failure does not propagate to the ground surface. The kinematic approach of limit analysis is used, and a brief discussion is presented about when the plasticity approach is acceptable for assessing the stability of the rock structures. An early plasticity approach to stability of a cavity roof was presented by Lippman (1971), who used both the static and kinematic approaches of limit analysis. Fraldi and Guarracino (2009) used the plasticity method with the variational approach to determine the shape of the long cavity (tunnel) failure mechanism, but they did not focus on measures of stability. Similar techniques were employed by Yang and Huang (2013) and Huang et al. (2014), while a numerical approach was considered by Suchowerska et al. (2012). Park and Michalowski (2019, 2020) used kinematic limit analysis to predict the measures of stability of roof cavities, with a focus on tunnels with curved ceilings, and they considered both 2D and 3D mechanisms of collapse.

There is considerable experience in application of limit analysis to metals and soils, but application of the method to rocks has received less attention. This is because rocks conform to strength criteria that are not linear functions of the mean stress, which causes some difficulties in using kinematic limit analysis. We focus first on the strength criteria used for rocks; in particular, we will focus on the Mohr-Coulomb criterion modified by a tension cut-off, and on the Hoek-Brown criterion. In the second part of the presentation, specific applications of the method are shown for considering stability of roofs in flat-ceiling cavities.

## ROCK STRENGTH CRITERIA AND PLASTIC ANALYSIS

Plasticity analysis is applicable to materials that exhibit ductile behavior, at least in some range of deformation after reaching the limit state (strength envelope). Experimental evidence supports some plasticity in rocks prior to failure (Mogi 1974), and plasticity analysis of rock failure has been used for decades. The early criterion used was the Mohr-Coulomb function modified with a tension cut-off (Drucker and Prager 1952; Paul 1961; Michalowski 1985, 2017).

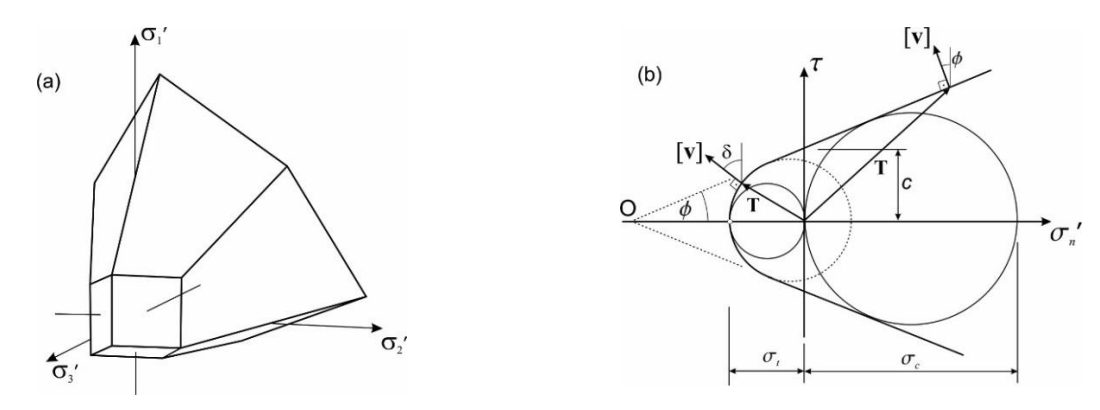


Figure 1. Mohr-Coulomb criterion with tension cut-off: (a) failure surface in Haigh-Westergaard space, and (b) strength envelope.

A Mohr-Coulomb failure surface with tension cut-off in the principal stress space is illustrated in Fig. 1(a), whereas the strength envelope on the τ-σ plane is shown in Fig. 1(b). Vectors [v] represent velocity discontinuity vectors along the failure surfaces (shear bands), consistent with the normality flow rule. The analytical description of this criterion can be found in Paul (1961). Its recent application to 3D analysis of safety assessment of rock slopes can be found in Park and Michalowski (2017). The strength criterion in Fig. 1(b) introduces the nonlinear dependence of the shear strength on the mean stress in the tensile regime. However, with further reduction in tensile strength, the nonlinear regime would reach the low-compression regime. The failure criterion preferred by many is one proposed by Hoek and Brown (1980, 2002) and illustrated in Fig. 2; therefore, the roof stability analysis will be carried out using the H-B strength envelope.

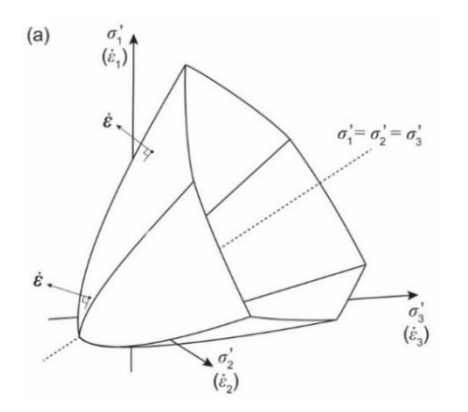
The Hoek-Brown failure criterion is expressed as a function of effective principal stresses

$$f(\sigma'_{ij}) = \sigma'_1 - \sigma'_3 - \sigma_{ci} \left( m_b \frac{\sigma'_3}{\sigma_{ci}} + s \right)^a = 0$$
 (1)

where  $\sigma'_1$  and  $\sigma'_3$  are the major and minor effective principal stresses (convention  $\sigma'_1 \geq \sigma'_2 \geq \sigma'_3$  relates to only one section of the surface in Fig. 2(a)), and  $\sigma_{ci}$  is the compressive strength of the intact rock. Parameters  $m_b$ , a, and s are dependent on Geological Strength Index GSI and disturbance factor D

$$m_b = m_i \exp\left(\frac{GSI - 100}{28 - 14D}\right), \qquad a = \frac{1}{2} + \frac{1}{6}\left(e^{-\frac{GSI}{15}} - e^{-\frac{20}{3}}\right), \qquad s = \exp\left(\frac{GSI - 100}{9 - 3D}\right)$$
 (2)

where  $m_i$  is a coefficient dependent on the type of rock (Hoek et al., 2002). As opposed to the Mohr-Coulomb criterion, the Hoek-Brown failure surface in the principal stress space does not consist of planar segments, and it has a curvature in both the meridional and octahedral cross-sections. The failure envelope in the  $\tau$ - $\sigma_n$  plane is curved in its entire range.



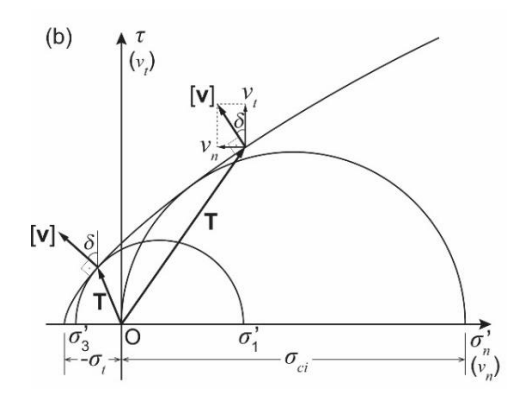


Figure 2. Hoek-Brown strength criterion: (a) Haigh-Westergaard space, and (b) strength envelope on  $\tau$ - $\sigma_n$  plane.

The kinematic approach of limit analysis is based on constructing a failure mechanism of a structure, which conforms to the normality plastic flow rule, with the plastic strain rate

$$\dot{\varepsilon}_{ij}^{pl} = \dot{\lambda} \frac{\partial f}{\partial \sigma_{ij}} \tag{3}$$

where  $f(\sigma'_{ij}) = 0$  is the failure criterion, and  $\lambda$  is the plastic multiplier (not a material property). If a failure pattern consists of rigid blocks separated by narrow failure zones (shear bands), often interpreted as failure surfaces, the normality flow rule can be written in terms of velocity discontinuity vector  $[v]_i$  and failure envelope  $f(T_i) = 0$  expressed as a function of stress vector  $T_i(\tau, \sigma_n)$  illustrated in Figs. 1(b) and 2(b)

$$[v]_i = \dot{\lambda} \frac{\partial f}{\partial T_i} \tag{4}$$

While the analyses for linear failure envelopes are straightforward, the nonlinearity in the Hoek-Brown criterion introduces some intricacies, because the failure criterion in Eq. (1) cannot be transformed easily into a function of the stress vector on the failure surface,  $f(T_i) = 0$ .

The kinematic approach is based on using the kinematic theorem of limit analysis. This theorem states that the rate of dissipated work in any kinematically admissible failure mechanism is not less than the work rate of true external forces

$$\int_{L} T_{i}[v]_{i} dL \ge \int_{V} X_{i} v_{i} dV + \int_{S} p_{i} v_{i} dS$$
(5)

where the term on the left side is the rate of dissipated work on failure surfaces L (no dissipation within the rigid blocks), and the terms on the right represent the work rate of distributed load  $X_i$  (weight) within volume V, and the work of roof supporting stress  $p_i$  (if any) on ceiling surface S.

When applying the theorem in Eq. (5) to stability problems, the inequality is replaced with the equation

$$D = W_{\gamma} + W_{p} \tag{6}$$

with D being the rate of work dissipation,  $W_{\gamma}$  is the work rate of gravity force, and  $W_p$  is the work rate of supporting stress p. Consequently, Eq. (6) will yield a bound to the true solution. If an active load causing failure is sought, Eq. (6) will yield an upper bound to the true solution, but if a passive force is searched for (such as supporting pressure p), it will be a lower bound.

## ROOF STABILITY MEASURES FOR ROCK CAVITIES

Three measures of roof stability over cavities in rocks have been considered: stability number N, support pressure p needed to prevent roof collapse, and factor of safety F. Stability number N is a dimensionless group of parameters describing the properties of the rock and the geometry of the cavity. For cavities with rectangular roofs it is convenient to use the following dimensionless group

$$N = \left(\frac{\sigma_{ci}}{\gamma B}\right)_{crit} \tag{7}$$

where the material properties are compressive strength of the intact rock  $\sigma_{ci}$  and rock unit weight  $\gamma$ , and the geometry enters the group through width B of the cavity. While the dimensionless group  $\sigma_{ci}/\gamma B$  can be calculated for any existing cavity, subscript "crit" indicates that the stability number is the critical value of the group, *i.e.*, when failure of the roof is imminent. A similar group has been used in safety analyses of rock slopes (Li et al. 2008; Park and Michalowski 2021). The difference between the dimensionless group  $\sigma_{ci}/\gamma B$  for an existing cavity and its critical value is indicative of the safety margin.

The second measure of safety is pressure p needed to support the cavity roof in order to assure stability (limit equilibrium). This pressure will be reported as dimensionless parameter  $p/\gamma B$ .

The third measure of safety/stability is factor of safety F

$$F = \frac{\tau}{\tau_d} \tag{8}$$

where  $\tau$  and  $\tau_d$  are the rock shear strength and the minimum demand on the shear strength to maintain stability, respectively. A graphical illustration of the rock shear strength reduced by factor of safety F (shear strength demand) is found in Fig. 3.

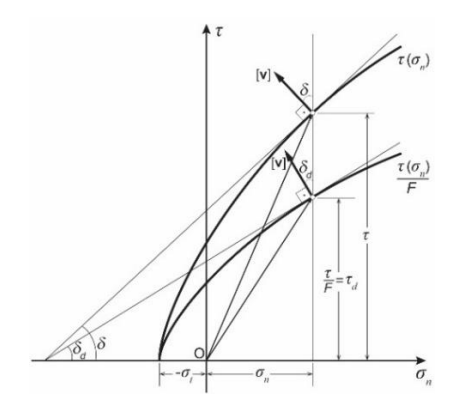


Figure 3. Nonlinear shear strength envelope  $\tau(\tau_n)$  reduced by factor of safety F.

Although used widely in assessment of safety of soil slopes, it is not as commonly used in rock mechanics. Presumably, this is because of intricacies associated with calculations of F for structures in rocks with strength governed by a nonlinear strength criterion, such as that in Eq. (1), in particular, the calculations of the rate of dissipated work. Consequently, attempts at defining the factor of safety by factoring the rock uniaxial compressive strength, rather than the shear strength, can be found in the literature (Li et al. 2008). While such a definition greatly simplifies the calculations, the factor of safety so defined differs from the commonly accepted definition in Eq. (8).

The rate of the work dissipation on failure surfaces L (in Eqs. (5) and (6)) can be written in general as

$$D = \int_{L} T_{i}[v]_{i} dL = \int_{L} [v] (\tau \cos \delta - \sigma'_{n} \sin \delta) dL$$
 (9)

where [v] is the magnitude of the velocity jump on failure surface L, and  $\delta$  is the rupture angle illustrated in Fig. 3. Because the Hoek-Brown condition cannot be written as explicit function  $f(\tau, \sigma'_n) = 0$ , a parametric representation of the function in Eq. (1) (Kumar 1998)

$$\sigma'_{n} = \sigma_{ci} \left\{ \left( \frac{1}{m_{b}} + \frac{\sin \delta}{m_{b} a} \right) \left[ \frac{m_{b} a (1 - \sin \delta)}{2 \sin \delta} \right]^{\frac{1}{1 - a}} - \frac{s}{m_{b}} \right\}, \quad \tau = \sigma_{ci} \left\{ \frac{\cos \delta}{2} \left[ \frac{m_{b} a (1 - \sin \delta)}{2 \sin \delta} \right]^{\frac{a}{1 - a}} \right\}$$
(10)

was used in order to find components  $\sigma'_n$  and  $\tau$  in Eq. (9); this proved instrumental in calculations of the measures of roof stability.

# ROOF COLLAPSE MECHANISMS IN ROCK CAVITIES

The short format of this paper does not allow presentation of the details of the failure mechanisms used in the calculations, nor the details of the numerical procedures. Therefore, in this section we present only a short overview of the geometry of the failure mechanism used. The mechanism considered consists of a rigid block moving down into the cavity. Before the block

separates from the stationary rock above, a thin layer between the moving block and the stationary rock is subjected to plastic deformation with a large shear component. This thin layer is illustrated in Fig. 4(a) by surface  $B_1B_{n+1}CB_1$ .

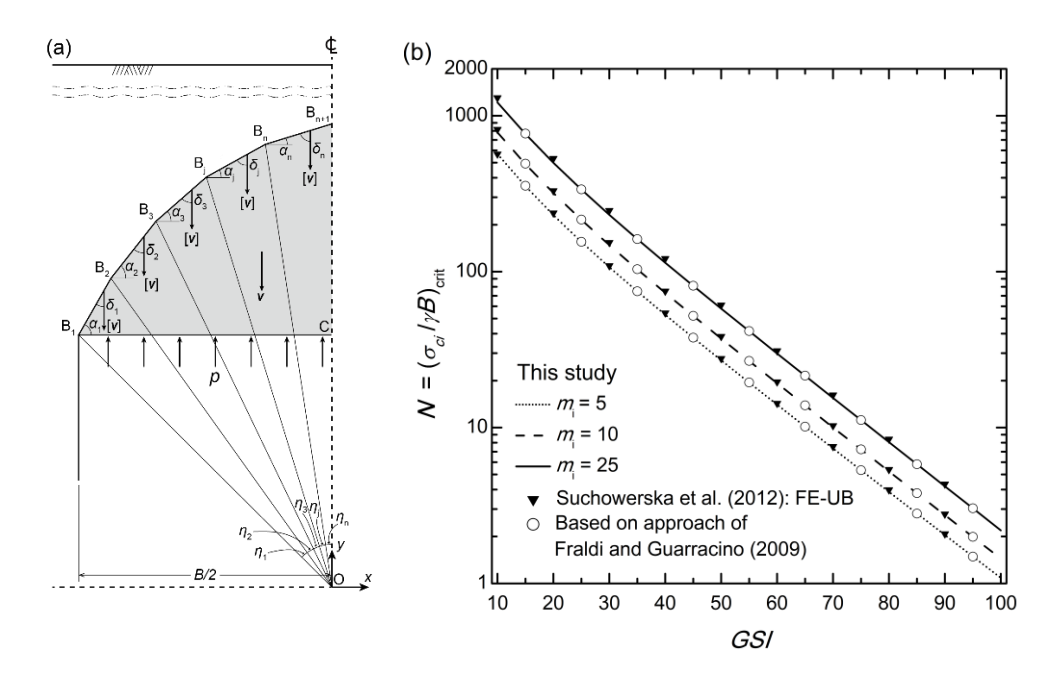


Figure 4. Flat-ceiling in a long cavity (tunnel): (a) symmetric half of failing block B<sub>1</sub>B<sub>n+1</sub>CB<sub>1</sub>, and (b) stability numbers (after Park and Michalowski, 2019) and comparison to existing results.

A characteristic feature of kinematic admissibility of the mechanism is the velocity discontinuity vector [v] being inclined at rupture angle  $\delta$  to the failure surface, as illustrated in Fig. 4(a). This is the consequence of the normality flow rule used in limit analysis. While the entire block moves as a rigid body, angle  $\delta$  is different on each surface segment  $B_1B_2$ ,  $B_2B_3$ , etc. This allows one to identify stress vector T along segments of the rupture surface (B<sub>1</sub>B<sub>2</sub>, B<sub>2</sub>B<sub>3</sub>, etc.), by finding the respective points with the same rupture angle  $\delta$  on the failure envelope, Fig. 2(b). Consequently, rate D of internal (dissipated) work in Eq. (6) can be calculated easily using Eq. (9). Rate of gravity work  $W_{\nu}$  is equal to the product of the weight of the failing block and velocity v of the block (equal to [v]). After substituting the two rates into Eq. (6) and some algebraic transformation, one can obtain stability number N for a long cavity (tunnel). Angles  $\alpha_i$ (j = 1, 2...n, n = number of segments) and  $\eta_i$  (j = 1, 2...n-1) in Fig. 4(a) are independent variables, and the mechanism was optimized to obtain the best (highest) estimate of N (the method yields a lower bound to N). This method was used in an analysis of a tunnel in rock governed by the M-C criterion with tension cut-off (Park and Michalowski 2018). This 2D solution will now be utilized as a part of a new 3D analysis to solve for the roof stability of a cavity with a rectangular ceiling.

The failure surface of the roof over a rectangular cavity is illustrated in Fig. 5(a) and its top view is shown in Fig. 5(b). The rock block defined by the surface in Fig. 5 is a right elliptical cone with a piece-wise linear generatrix. The two halves of the elliptic cone are separated with a centric "insert" constructed similarly to that in the 2D analysis illustrated in Fig. 4(a).

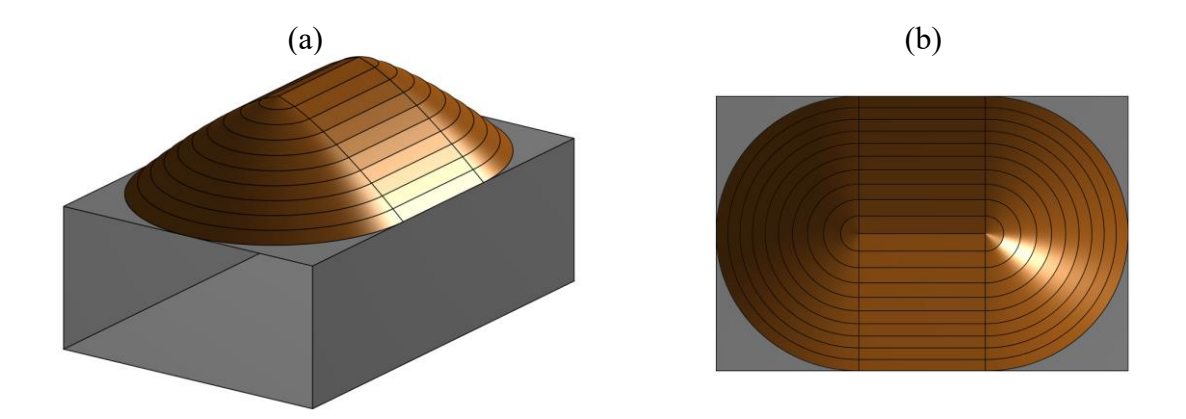


Figure 5. Composite failure surface in the roof over a cavity with rectangular ceiling: (a) side view, and (b) top view.

The right elliptic cone is described with the following equation (the origin of the coordinate system is at the level of the cavity ceiling):

$$\frac{x^2}{a^2} + \frac{y^2}{b^2} = \frac{(z - h)^2}{h^2}$$
 (11)

where a and b are the half-axes of the cone base, and h is the cone height. The elliptic cone in Fig. 5 consists of a series of n frusta of cones with varied height and half-axes, but with the same ratio  $\lambda = b/a$  for each cone. The two halves of the cone are separated by an insert with 2D geometry as in Fig. 4(a). Introducing inclination angle  $\alpha_j$  of the generatrix of cone slice or frustum j (j = 1, 2...n), defined as  $\tan^{-1}(a/h)$ , Eq. (11) can be rewritten for each frustum j (horizontal slice in Fig. 5) as

$$x^{2} + \frac{y^{2}}{\lambda^{2}} = \frac{(z - h_{j})^{2}}{\tan^{2} \alpha_{i}}$$
 (12)

Based on this description of the geometry, one can develop analytical expressions for the areas of the frusta and their volumes. The former is needed to describe the rate of work dissipation during failure, and the latter for the rate of gravity work. These expressions were combined with the respective rates for the 2D central insert, substituted in Eq. (6), and expressions for stability number N, dimensionless supporting pressure  $p/\gamma B$ , and an implicit equation for the factor of safety were developed.

# **COMPUTATIONAL RESULTS**

The expressions for the stability number, supporting pressure, and the implicit expression for the factor of safety are all functions of independent variables  $\alpha_j$  (j = 1, 2...n) and  $\eta_j$  (j = 1, 2...n) illustrated in Fig. 4(a), and aspect ratio  $\lambda$  of the right elliptic cone, Eq. (12). Notice that  $\lambda$  is not equal to the cavity ceiling aspect ratio L/B, because length L includes not only the half-axes of the ellipse, but also the length of the insert, as illustrated in Fig. 5.

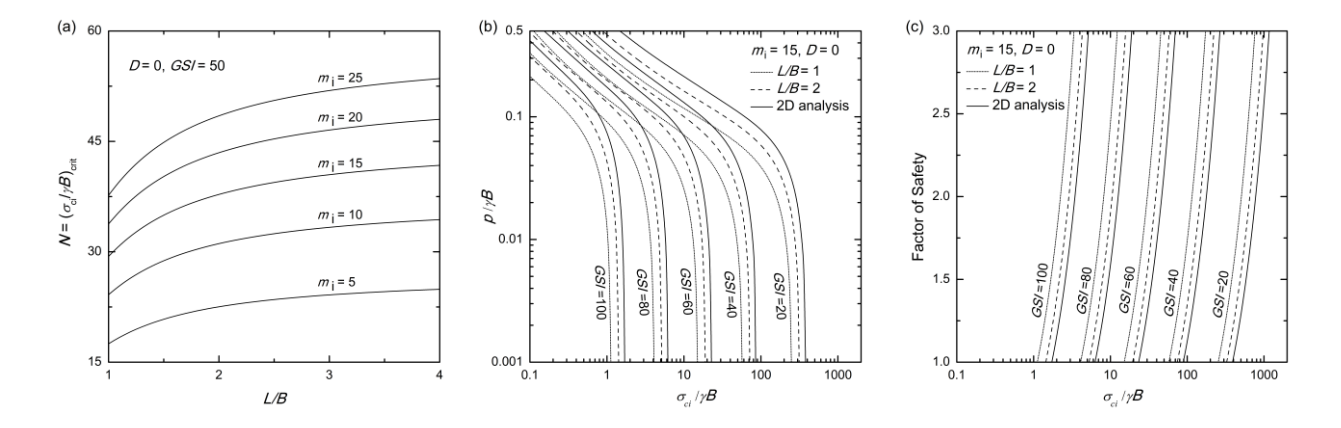


Figure 6. Computational results for a 3D failure pattern (shown in Fig. 5): (a) stability number N as function of ceiling aspect ratio L/B and rock type parameter  $m_i$ , (b) minimum supporting pressure as function of group  $\sigma_{ci}/\gamma B$ , aspect ratio L/B, and GSI, and (c) factor of safety.

Calculated stability number N for a minimally disturbed rock, D = 0, with GSI = 50, is shown in Fig. 6(a). The calculations were performed assuming the roof is not supported with pressure p, thus the second term in Eq. (6) was taken as zero in the development of the expression for N. As the kinematic limit analysis yields the lower bound to the stability number, a set of angles  $\alpha_j$  (j = 1, 2...n) and  $\eta_j$  (j = 1, 2...n-1) and  $\lambda$  were varied until the maximum value of N was found. The stability number is shown as a function of the aspect ratio of cavity ceiling L/B for a variety of rock parameters  $m_i$ . Of rectangular-ceiling cavities the most stable are the ones with square ceilings (L/B = 1). This result was intuitively expected. Surprisingly, the stability factor increases with an increase in  $m_i$ . This issue was discussed earlier in the context of deep tunnels (Park and Michalowski 2019); while the rock shear strength expressed in the Hoek-Brown criterion increases for large confining stresses with an increase in parameter  $m_i$ , for low confining stresses (such as those in roof stability analyses), the trend is opposite. Hence the surprising outcome.

Fig. 6(b) illustrates dimensionless minimum support pressure p, needed to prevent cavity roof collapse in relatively weak rocks (cases where the cavity will not be stable without supporting pressure). Supporting pressure p is illustrated in Fig. 4(a). This time, the last term in Eq. (6) is included in the analysis. The supporting pressure is the reaction of a supporting structure to the rock load (leading to negative work rate  $W_{\gamma}$ ); therefore, the kinematic approach yields the lower bound to p, and the maximum of p was sought in the analysis with angles  $\alpha_j$  (j = 1, 2...n) and  $\eta_j$  (j = 1, 2...n1) and ratio  $\lambda$  being independent variables. The results are shown for cavity ceiling aspect ratios 1, 2, and for a long cavity (2D analysis), as functions of the uniaxial compressive strength of the rock (dimensionless). Not surprisingly, the weaker the rock the larger the pressure needed to keep the cavity roof stable (note the log scale).

Finally, the plot with factor of safety F, as defined in Eq. (8), is shown in Fig. 6(c). The kinematic approach yields the upper bound to F; therefore, a minimum F was sought with  $\alpha_j$  (j = 1, 2...n),  $\eta_j$  (j = 1, 2...n-1), and ratio  $\lambda$  being independent variables. Not surprisingly, for a given GSI, the factor of safety increases rapidly with an increase in the rock strength (note the semi-log plot).

#### CONCLUSIONS

The plasticity approach to stability of rock structures is based on the premise that upon reaching the limit state, rock will plastically deform before a brittle drop off in the stress. Three roof stability measures were evaluated for deep cavities in rock with strength governed by the Hoek-Brown failure criterion. This failure criterion cannot be transformed into the shear strength envelope of the form  $f(\tau, \sigma'_n) = 0$ , and the analytical development of the expressions for the stability measures was made possible thanks to a parametric representation of the H-B strength criterion.

Stability number N is a useful measure indicating the margin of safety by comparing it to the actual dimensionless group  $\sigma_{ci}/\gamma B$ ; the larger the difference the larger the safety margin and the smaller the dimensionless group the less stable the cavity roof. Stability number N is strongly dependent on the properties of the rock and the geometry of the cavity, but only limited results could be presented in this short paper.

Large cavities or cavities in weak rock require a support pressure in order to remain stable. This support pressure is strongly dependent on the rock strength and the quality of rock articulated in Geological Strength Index (GSI). Finally, the factor of safety is perhaps the most intuitive measure of the stability of cavity roofs in rock. It is very much dependent on the strength of the rock relative to the cavity size and the quality of the rock expressed in GSI.

# **ACKNOWLEDGEMENTS**

The work presented in this paper was carried out while the authors were supported by the National Science Foundation, Grant No. CMMI-1901582, and the Horace Rackham School of Graduate Studies at the University of Michigan. The work was also supported by the National Research Foundation of Korea (NRF) grant funded by the Korea government (MSIT), No. 2021R1G1A1003943. This support is greatly appreciated.

## REFERENCES

- Drucker, D. C., and Prager, W. (1952). "Soil mechanics and plastic analysis or limit design." *Quart. Appl. Math.*, 10(1), 157-165.
- Fraldi, M., and Guarracino, F. (2009). "Limit analysis of collapse mechanisms in cavities and tunnels according to the Hoek–Brown failure criterion." *Int. J. Rock Mech. Min. Sci.*, 46(4), 665-673.
- Hoek, E., Carranza-Torres, C., and Corkum, B. (2002). "Hoek-Brown failure criterion-2002 edition." *Proceedings of NARMS-Tac.*, 267-273.
- Hoek, E., and Brown, E. T. (1980). "Empirical strength criterion for rock masses." *J. Geotech. Eng. Div.*, 106(9), 1013-1035.
- Huang, F., Yang, X., and Ling, T. (2014). "Prediction of collapsing region above deep spherical cavity roof under axis-symmetrical conditions." *Rock. Mech. Rock Eng.* 47(4): 1511-1516.
- Kumar, P. (1998). "Shear failure envelope of Hoek-Brown criterion for rockmass." *Tunn. Undergr. Space Tech.*, 13(4), 453-458.
- Li, A., Merifield, R., and Lyamin, A. (2008). "Stability charts for rock slopes based on the Hoek–Brown failure criterion." *Int. J. Rock Mech. Min. Sci.*, 45(5), 689-700.
- Lippmann, H. (1971). "Plasticity in rock mechanics." Int. J. Mech. Sci., 13(4), 291-297.

- Michalowski, R. L. (1985). "Limit analysis of quasi-static pyramidal indentation of rock." *Int. J. Rock Mech. Min. Sci.*, 22(1), 31-38.
- Michalowski, R. L. (2017). "Stability of intact slopes with tensile strength cut-off." *Géotechnique*, 67(8), 720-727.
- Michalowski, R. L., and Park, D. (2020). "Stability assessment of slopes in rock governed by the Hoek-Brown strength criterion." *Int. J. Rock Mech. Min. Sci.*, 127(March), 104217(1-12).
- Mogi, K. (1974). "On the pressure dependence of strength of rocks and the Coulomb fracture criterion." *Tectonophysics*, 21(3), 273-285.
- Park, D., and Michalowski, R. L. (2017). "Three-dimensional stability analysis of slopes in hard soil/soft rock with tensile strength cut-off." *Eng. Geology*, 229, 73-84.
- Park, D., and Michalowski, R. L. (2018). "Tunnel roof stability in soft rock with tension cutoff." *GeoShanghai International Conference*, Shanghai; 27–30 May 2018, pp. 361-368.
- Park, D., and Michalowski, R. L. (2019). "Roof stability in deep rock tunnels." *Int. J. Rock Mech. Min. Sci.* 124(December), 104139(1-12).
- Park, D., and Michalowski, R. L. (2020). "Three-dimensional roof collapse analysis in circular tunnels in rock." *Int. J. Rock Mech. Min. Sci.*, 128(April), 104275(1-12).
- Park, D., and Michalowski, R. L. (2021). "Three-dimensional stability assessment of slopes in intact rock governed by the Hoek-Brown failure criterion." *Int. J. Rock Mech. Min. Sci.*, 137(Jan.), 104522 (1-13).
- Paul, B. (1961). "A modification of the Coulomb-Mohr theory of fracture." *J. Appl. Mech.* 28(2): 259-268.
- Suchowerska, A. M., Merifield, R. S., Carter, J. P., and Clausen, J. (2012). "Prediction of underground cavity roof collapse using the Hoek–Brown failure criterion." *Comput Geotech.*, 44, 93-103.
- Yang, X., and Huang, F. (2013). "Three-dimensional failure mechanism of a rectangular cavity in a Hoek–Brown rock medium." *Int. J. Rock Mech. Min. Sci.*, 61, 189-195.